Journal of Building Engineering 103 (2025) 112149

Contents lists available at ScienceDirect

Journal of Building Engineering

journal homepage: www.elsevier.com/locate/jobe

Identifying the alteration in the thermal properties of aerogel thermal insulation after heat treatment with different methods

Ákos Lakatos [a,*], Attila Csík [b], Petra Herman [c], István Csarnovics [d]

[a] University of Debrecen Faculty of Engineering, Department of Building Services and Building Engineering, Ótemető Str 2-4, Debrecen, H-4028, Hungary
[b] HUN-REN Institute for Nuclear Research, Bem tér 18/c, H-4026, Debrecen, Hungary
[c] HUN-REN-DE Mechanisms of Complex Homogeneous and Heterogeneous Chemical Reactions Research Group, Department of Inorganic and Analytical Chemistry, University of Debrecen, Egyetem tér 1, Debrecen, H-4032, Hungary
[d] University of Debrecen, Faculty of Science and Technology, Institute of Physics, Department of Experimental Physics, Hungary

ARTICLE INFO

Keywords:
Aerogel
Heat stability
Spectroscopy
Thermal properties

ABSTRACT

Regulations aimed at limiting and eliminating unnecessary energy usage and the associated emissions of hazardous materials are becoming more and more stringent when it comes to newly planned and built buildings. The need for these initiatives is also growing among consumers due to the rise of an increasingly environmentally and energy-conscious mindset. Moreover, vehicles, industrial applications, or pipes transporting hot water can also use thin layered insulation.

Aerogel materials fit these cases, too. Technological advances have also led to an expansion in the production of thermal insulation materials. New materials like aerogels, vacuum thermal insulation panels, and graphite-infused polystyrene foam have joined the market. It is essential to understand their properties after aging them through heat treatments. This study presents the change in the thermal properties of a Pyrogel-type aerogel material after thermal treatment at 150 and 250 °C for 1 day. The reason for this was to understand the thermal stability of the samples for their possible use at a temperature range of up to 250 °C. Because, in some cases, these materials can meet higher temperatures, such as in industrial cases. Due to the thermal annealing, the thermal conductivity, diffusivity, and volumetric heat capacity change will be discussed. We deduced a 5 % increase in thermal conductivity and a 6 % increase in the specific heat capacity after thermal annealing at 250 °C. These characteristics resulted in changes in thermal diffusivity and the volumetric heat capacity. The thermal diffusivity changed only after annealing at 250 °C, while the volumetric heat capacity continuously increased.

Micro and macrostructural characterization tests were executed on the samples to understand this. Moreover, the microscopic background of these changes is also revealed. Several complementary measurements were used to explain the changes, such as X-ray diffraction, differential scanning calorimetry, infrared spectroscopy (IR), and Raman spectroscopy. The test methods have demonstrated that the observed increases in thermal conductivity, specific heat, and volumetric heat capacity are primarily due to significant crystallization and recrystallization processes occurring within the aerogel material. Additionally, the slight alteration in thermal diffusion is linked to amorphization, indicating a complex interplay between structural changes and thermal properties. This nuanced understanding highlights the importance of thorough characterization in evaluating the behaviour of materials under varying thermal treatments. These measurements

* Corresponding author.
E-mail address: alakatos@eng.unideb.hu (Á. Lakatos).

https://doi.org/10.1016/j.jobe.2025.112149
Received 16 November 2024; Received in revised form 5 January 2025; Accepted 16 February 2025
Available online 20 February 2025

also gave results on crystallization and amorphous changes as an explanation of the thermal changes. The interdisciplinarity of our paper proves its innovation. We briefly presented the environmental impact of aerogels.

1. Introduction

The building industry plays a significant part in greenhouse gas emissions, and the energy use of residential and commercial structures often drives the research and development of high-performance thermal insulations. The energy consumption of the building sector is increasing and may eventually overtake other sectors, like industry. Enhancing the thermal insulation of the buildings is a frequent method used in the European Union (EU) to use net zero energy buildings (NZEBs) to meet sustainability targets for 2050 [1–8]. Energy requirements for heating and cooling can be reduced by up to 50 % with proper insulation, which results in significant drops in greenhouse gas emissions. It is presented in Ref. [9] that lignocellulose-based insulation materials or bios-based insulations from wastes and renewables are eco-friendly solutions. This method allows renewable materials to be substituted for 30–50 % of the polymer content, consistent with sustainability ideals. Moreover, the thermal conductivity of their forms is within the same range as the plastic-based ones [10].

Furthermore, In Ref. [11], it is also presented that agricultural waste is also a proper material from a sustainability point of view. The literature [12–14] states that between 60 and 65 percent of the insulation materials available on the market are inorganic (mineral wool), 21 percent are organic, and the remaining portion is novel and composite materials such as aerogels and vacuum insulation panels. These two have much lower thermal conductivity than the above-mentioned ones. Various thermal insulation materials have recently been created with the concepts of environmental preservation, increased energy efficiency, and global sustainability in mind [15].

Additionally, thermal insulation is vital for building envelopes, and their use for building service types of equipment is also necessary. Developing building service systems that improve the building's efficiency is therefore urgently needed. This is why novel materials are crucial, as they can be applied in thin forms and stand at high temperatures [15].

Regarding insulating materials, aerogels and other super-insulators are outstanding and suitable methods. Although advanced or nanostructured thermal insulation materials are also often used terms to describe aerogel materials, the term "super thermal insulation material" is now also used, which comes from the term "Super Insulation Material (SIM)". Super-insulating materials, a recently developed category of these goods, have the potential to be crucial to insulation in the future.

Although the term "SIMs" lacks a specific definition, the elements of this group are defined in Annex 65 of the IEA EBC (International Energy Agency, Energy in Buildings and Communities Programme). Per this appendix, the following are included in the group: Vacuum thermal insulation panels, or VIPs; b) unique porous materials, like different kinds of aerogels (fibrous or monolithic). These materials have gained popularity as attractive substitutes for conventional thermal insulation materials that are used internally and have insulation thickness lowered by half to a third. Products made of silica aerogel are frequently considered materials that show promise for raising the building envelope's thermal resistance. Notwithstanding their exceptional insulating capabilities, these materials come at a very high cost, and scant information regarding their longevity, intermediate performance, and fundamental thermal characteristics is available. Examining the thermomechanical properties of the materials listed, including determining these parameters, is one of the main focuses of this research, especially concerning fibrous silica aerogel. This problem must be solved since the databases that summarize newly created materials' specific heat and thermal conductivity coefficients are frequently ambiguous or lack information.

Furthermore, it often occurs that the lambda values provided by the manufacturers differ from the outcomes of the tests conducted in the laboratory. There is regularly insufficient information about thermal insulation materials to fully understand how certain external conditions, like moisture, temperature, or age, can alter their properties, possibly even their structure. The critical point is how environmental factors cause them to lose their properties over time and how the good thermal insulation qualities that exist during production deteriorate. Moreover, nothing is understood about their behaviour when analyzed because of their fundamental structures [16–18]. The authors state that aerogels are one of the lowest thermal conductivity materials that can be used for thermal insulation. They can also be used as composites with epoxy [19–21]. Due to their nature, aerogels are often strengthened with other materials, such as plastic components like polyurethane. The composite materials are new, so thermal investigations are necessary [22]. Moreover, it is justified that aerogel thermal insulation can be well applied in hot environments. Nanoporous carbon aerogel performs well as thermal insulation in harsh environments because of its exceptional qualities, including low thermal conductivity and ultra-high temperature resistance. It makes an excellent choice for ultra-high temperature thermal insulation in aircraft thermal protection systems and for hot places such as power plant applications and chimneys [23,24]. This is why investigating their properties under extreme environmental conditions is crucial. These can be simulated by thermal treatments or ageing [25–28].

These encounters served as the foundation for the research project and justified performing the examinations. Due to their high porosity and low density, aerogels have been utilized as lightweight materials in a variety of applications, such as the aerospace and equipment industries, since the introduction of novel materials in recent years [29,30], and [31].

A 10–40 % reduction may be achieved using aerogels from the heat loss through the walls [32–35]. Moreover, their use as insulating building services systems, equipment, and pipes reduces energy loss. The research carried out on the thermal insulation samples covered the assessment of the thermal insulation capacity, diffusivity factor, and volumetric heat capacity because these parameters are decisive in the usability of the insulation materials. This study will present the study of the change in thermal parameters due to

heat treatment and show a comprehensive experimental research row to support each other for revealing the microscopic and macroscopic changes inside the material.

Both thermal and microstructural characterization are significant for building materials. The authors investigate their materials using novel solid-state physical methods, such as XRD, FTIR, and DSC, similar to the current study. They also show whether different methods can support each other to entirely understand the thermos-mechanical changes of building materials [36]. Rahimzedah et al. also presented that plaster made of lime is commonly used as a thermal insulator in building construction. In Ref. [37], the authors present experiments on heat treatment and water sorption, a microstructure analysis, and modelling of the compression stress-strain behaviour of screed paste and roofs made of lime. It is also notable that Rahimzadeh and his colleagues showed that the pastes made of lime are incredibly intricate constructions of several mortars. Lime-based screed or paste is frequently utilized as a thermal insulator in buildings. Because they shield buildings from the elements and affect occupant thermal comfort, screeds are essential envelope building materials. They also applied multiple experiments to investigate thermal insulation materials. Besides DSC, XRD, and FTIR experiments, they also used thermogravimetry, scanning electron microscopy, sorption, and compressive strength experiments [38]. In contrast to their papers, we also made experiments to see the changes in the thermal insulation capability.

The pyrogel aerogel insulations evaluated are relatively recent and have a wide range of applications in the industry. The large-scale production of pyrogel aerogels is available from manufacturers. These materials can be found in a couple of thickness centimetres and blanket form. In some cases, such as in industry or power plants, having pipes transporting hot water pyrogel can be satisfactory insulation. Because it may forecast the insulation's lifespan and application limit, thermal annealing - which also describes the samples' thermal ageing - is crucial. The research's interdisciplinarity is another innovative aspect. The basis of the structural alterations and associated processes was revealed by rigorous solid-state physical examinations and the study's general building physical investigations (specific heat and thermal conductivity). The following is where the paper's novelty lies.

1.1. Aims and hypotheses

Investigating the suitability and effectiveness of pyrogel aerogel insulation material as a possible thermal insulator in thin forms for buildings/vehicles (not thermal annealed form) and industrial applications (after thermal annealing) is the goal of this multidisciplinary study.

The article's significant hypotheses are as follows:

a) Does the pyrogel material's appearance alter due to heat treatment at 150 and 250 °C in the air?
b) Does heat treatment alter the pyrogel material's structure?
c) Has the pyrogel material's structure changed, and if so, how does this impact its thermal properties, including volumetric heat capacity, specific heat, diffusivity, and thermal conductivity?

2. Materials and methods

2.1. Methodology

This study combines analytical and experimental methodologies to assess the thermal performance and the structural integrity of the pyrogel insulating material. The experimental protocols and data analysis carried out are delineated in the subsequent steps:

- Presentation of the thermal conductivity of porous materials (section 2.2).
- Presentation of thermal degradation and heat treatment (sections 2.8, 3.1.)
- Presentation of thermal conductivity and specific heat measurements (sections 2.3, 3.2).
  - o Investigation of the alteration of thermal diffusivity and volumetric heat capacity after heat treatment (section 3.3).
- 2.4. Differential Scanning Calorimetry (sections 2.4, 3.5.).
- X-ray diffractometry (sections 2.5, 3.4).
- 2.6. Investigation of the bond structure of the samples (FT-IR, Raman) (sections 2.6, 3.6).
- Tested aerogel material as pyrogel, and comparison with graphite EPS and vacuum insulation panels (section 2.7).
- Environmental impact (section 3.7)

2.2. Thermal conductivity of the porous materials

The thermal conductivity factor is one of thermal insulation materials' critical thermal technical properties. Its thermal conductivity measures how quickly heat can move through a material by conduction. Conduction is the primary heat transfer method through insulation. The value is commonly called the λ (lambda, W/mK). The performance is better when the value is smaller. During production, efforts should be made to maintain this value as low as possible once the product is installed. Variations in temperature and humidity can impact the components of a building's thermal envelope, leading to a decline in the building's structural integrity. For engineers to work with accurate values during planning, the thermal conductivity factor and moisture absorption capacity of thermal insulation materials must be examined in a laboratory. Specific data are available in tabular form in various open-access literature and manufacturer brochures [30,31]. Most are very useful, but we often find incorrect or incomplete information. In the case of materials, it is necessary to enter not only the thermal conductivity coefficient correctly but also, for example, the density, pressure or moisture

content, and temperature at which the thermal conductivity coefficient was determined. In addition, it is also essential to know their additional thermal properties, such as the specific heat or heat of combustion. To specify the thermal conductivity of the materials accurately, it is vital to know the time since production and the storage method (air temperature and humidity).

Because high porosity material prevents phonons from propagating in the aerogel's backbone, heat conduction through the solid framework reduces as porosity rises. Elastic collisions between gas molecules explain the contribution of the gas phase. The gas phase's thermal conductivity depends on the pores' size and the average accessible route length of the gas molecules inside them. For aerogel to be an effective thermal insulator, its thermal conductivity needs to be lower than that of "free" ambient air (0.025 W/mK at 300 K and 1 atm pressure) [39]. If the pore size is less than the typical accessible route length of air molecules (70 nm), the Knudsen effect, or the gas's thermal diffusion, may be inhibited. Reducing pressure is another way to accomplish this. The Knudsen number is the mean accessible route of gas molecules divided by the pore diameter. The pores' nanometric size lowers radiation, gaseous convective heat transfer, and conductive heat transmission [40,41]. The heat required to raise 1 kg of a material's temperature by 1 K (or 1 °C) is known as its specific heat capacity. It takes time for an excellent insulator to absorb more heat before the temperature rises and the heat is transferred. Hence, a good insulator has a larger specific heat capacity. Materials with a high specific heat capacity offer thermal mass or buffering (reduction delay) [42,43].

2.3. Thermal conductivity and specific heat capacity measurements

We tested the materials' thermal conductivity (λ) with a Netzsch 446 heat flow measuring device, which also allows for determining the specific heat capacity. Some of the essential advantages of this equipment are that, on the one hand, it measures the specific heat capacity (c, J/kgK) of the materials, and the heat conduction factor can be examined with an accuracy of approximately ±2 % even under different loads and compressive forces. The measuring instrument was designed using the following standards: ASTM C518, ISO 8301, JIS A1412, DIN EN 12664, and DIN EN 12667. The equipment measures the specific heat step by step, heating the sample while keeping the two plates at the same temperature. The equipment measures the specific heat between two fixed temperatures. The integral of the heat flow sensor signal in each step represents the total amount of heat entering or exiting the sample. The plates' specific heat capacity also influences this, but the apparatus takes this contribution into account. The 20 cm × 20 cm sample is positioned between two heated plates in the heat flow meter in the same manner as in the previously described apparatus. The sample's maximum thickness of 5 cm is only permitted here [17,18].

2.4. Differential scanning calorimetry

Differential scanning calorimetry is a popular technique for analyzing contaminants' release and potential sample alterations following heat supply. As a result, we used 10–20 mg mass to evaluate ground samples from the entire blanket. The following was the measurement order: The samples were heated from 30 to 350 °C with a heating rate of 10 °C/min in a concave aluminium piercing lid in a nitrogen environment with 40 and 60 ml/min flow (ambient and protected). The DSC sign (in MW/mg) was then recorded as a function of temperature. The potential energy and structural alterations were assessed based on the DSC grams. The Netzsch DSC Sirius 3500 equipment utilized for this measurement conforms with ASTM E793, ASTM D3895, DIN 51004, ISO 11357, and ASTM D3418 standards [44].

2.5. X-ray diffractometry investigations

The Rigaku SmartLab diffractometer was used to make X-ray diffraction (XRD) measurements using CuK-alpha irradiation with a wavelength of 0.154 nm to gather crystallographic information from the un-annealed and annealed samples. The samples were scanned in the 10-80° theta–2theta range using Bragg–Brentano focusing geometry to detect potential crystalline phase alterations. The X-Ray tube was operated with 45 kV, 200 mA parameters [44–46].

2.6. Investigation of the bond structure of the samples (FT-IR, Raman)

It was earlier presented in the Authors' paper in Refs. [47,48] that Raman spectroscopy is an accurate method to investigate the change in both the micro and macrostructure of aerogels after thermal annealing, especially for silica aerogels. Raman spectroscopy is a quantitative, species-specific, easy-to-use, and non-invasive spectroscopic technique [49,50]. It was also presented that Raman spectroscopy that the lattice vibration modes of the aerogels can be inferred from the Raman spectra [51,52].

FTIR (Fourier-transform infrared) and Raman spectroscopy provide molecular details on the makeup and structure of biological and chemical materials. Both technologies can produce complementary information because of their underlying principles. While Raman spectroscopy employs light in the visible, near-IR (NIR), or occasionally ultraviolet (UV) areas, usually around 785 nm, IR spectroscopy uses light energy over the entire infrared region of the electromagnetic spectrum. For this IR spectroscopy can supplement the results of Raman investigations well. The thermal characteristics of silica aerogel are characterized using an infrared emission spectroscopy spectrum technique. It offers spectral data on heat transfer [53]. Moreover, it was also presented that the physical characteristics of silica aerogels can be efficiently investigated using Fourier-transform infrared spectroscopy (FTIR) [54].

Ref. [55] also presents that FT-IR spectroscopy completed with XRD analysis can effectively investigate the structural change caused by thermal conductivity variation. In Ref. [56], the authors used the Fourier transform infrared spectrophotometer to examine the complexes' structure in the aerogel composite.

The pre–and after-annealing samples were investigated via Infrared (IR) and Raman spectroscopies to understand the changes in their bond structures due to heat treatment.

The Horiba LabRam spectrometer was utilized for the Raman spectroscopy investigations. It employed a cooled CCD detector and a laser diode with an operating wavelength of 532 nm. Because 600 lines/mm gratings were used for the measurement, the peak positions had an accuracy of at least $\pm 1.5\ cm^{-1}$. A 20x lens focused on the excitation beam onto the sample's surface. On the surface, the laser output was roughly 1 mW/cm^2. The measurement was performed with an acquisition time of 10 s, with an accumulation of 10. The measured spectra were analyzed, and the baseline corrected.

Besides, the samples were investigated using infrared spectroscopy to understand the bond structure changes [47,48].

The aerogel samples' infrared spectra (FT-IR) were measured in a PerkinElmer Spectrum Two Spectrometer using a universal ATR head (Single Reflection Diamond – L1600607). No sample pre-treatment was applied; representative 1 mm × 1 mm size aerogel pieces were directly attached to the probe. In order to support reproducibility, three samples were investigated from each (pristine and treated) aerogel panel. The IR spectra of the samples were recorded by averaging 8 scans in the spectral range of 550–4000 cm^{-1}. The experimental spectra were evaluated without using any mathematical transformations.

2.7. The tested aerogel material

As mentioned, the chosen thermal insulation materials discussed are glass fibre-reinforced silica aerogel. According to IEA Annex 65, this material belongs to the advanced porous products of superheat insulating materials. Before detailing the material's properties, it is essential to describe what advanced porous materials are. By this acronym, we mean materials with open pore architectures and nanostructures. Although this ratio is often between 90 and 94 %, their porosity can reach 97 %. Their density ranges from 50 to 250 kg/m^3. The names of aerogels are primarily inspired by their unique appearance, which can be frozen smoke, solid smoke and, finally, blue smoke. Preparing the silica sol for the solvent-containing gel as a first step is necessary [40]. During its production, the liquid is carefully removed from the silica-alcogel, and its place is filled with air; thus, the final product containing air is obtained. The aerogel thermal insulation quilt is a flexible composite material, which is an aerogel embedded in a glass fibre network. We tested pyrogel insulation, which can also be used for pipe insulation. The tested substance can be utilized safely in many aspects of life because of its non-toxic properties. It fits any place without losing its tensile strength or flexibility because it is plastic and slightly compressible. Its particles have modest contact surfaces with one another. The route length necessary for the free collision of gas molecules within the nanopores is greater than the size of the cavities within them. There is little convection heat flow because the gas molecules clash with the cavity walls. Many of the heat rays are reflected and scattered by the surface of the nanopores since their size is smaller than the wavelength of infrared heat rays. Different products have different thermal conductivity coefficients, but these values are average lower than still air's thermal conductivity coefficient or compared to plastic foam. Aerogel materials have declared thermal conductivity factors of 0.013–0.025 W/mK and have good light transmission and sound insulation capabilities. Due to its low thermal conductivity, aerogel can also be used as thermal insulation in smaller thicknesses. In recent years, several research groups have begun to deal with the thermomechanical properties of silica aerogel, paying particular attention to examining its moisture absorption properties and thermal conductivity [44–46].

2.7.1. The pyrogel-type aerogel

Because of its high carbon content and greenish-grey hue, pyrogel can be used as pipe insulation. Pyrogel industrial insulation has produced quantifiable benefits in many critical industrial and energy processes, including petrochemical, power plants, floating production, storage, offloading (FPSO), and refining. Aspen's industrial aerogel insulation is ideally positioned to support emerging energy solutions, further helping to meet the most rigorous ecological goals.

The novel hydrophobic design minimizes water absorption to optimize protection against corrosion under insulation (CUI) and corrosion under fireproofing (CUF). Long-lasting water resistance is ensured by pyrogel insulation for both the insulation layer and the underlying asset. Extended asset dryness preserves critical assets, saves energy, and maintains process conditions. Pyrogel offers unique characteristics and advantages to guarantee a reliable performance that satisfies requirements and performance objectives. Pyrogel thermal insulation material can be effectively used in industrial applications. This material stands till 650 °C. Applying amorphous silica and hybrid aerogels benefits pressing global challenges, including economic methods for carbon capture and the provision of clean water. This material can be used for both piping and building equipment. These flexible blanket insulations are suggested for piping, fittings, valves, flanges, and elbows. Through their industrial applications, they can meet high temperatures [57]. The aerogels' life cycle assessments and sustainability are well presented in Ref. [58]. In this study, the authors demonstrate that the

Table 1
Thermal properties of different insulation materials.

Thermal properties	Pyrogel [57]	Graphite EPS [59]	Vacuum insulation panel [60]
Thermal conductivity at 10 °C mean temperature [W/mK]	0.02 W/mK	0.032	Depending on the core materials and manufacturer Center of panel thermal conductivity 0.004-0.007
Compressive strength at 10 % strain [kPa]	102	80	Depending on the core material, usually silica-based as 100
Density [kg/m^3]	180–220	15–20	150–250
Fire resistance category [A1, A2, B, C, D, E, F, A1-best, F-worst]	A1	E	Depending on the core material, usually silica-based as A1.

aerogel material's environmental impact and the potential for global warming are highly variable. We obtained the samples from a distributor and did not produce them.

2.7.2. Comparison of the thermal properties of pyrogel insulation with graphite EPS and vacuum insulation panels

In Table 1, we collected the most important thermal properties of pyrogel aerogel, graphite EPS and vacuum insulation panels. We compared the thermal conductivities, compressive strength densities and the fire resistance.

The table shows that the thermal properties of graphite EPS are worse than those of aerogels and vacuum panels in all cases. At the same time, the thermal conductivity of vacuum panels is the lowest.

2.8. Thermal degradation of materials

Materials undergo aging, which causes gradual changes to their mechanical, thermal, and physical characteristics. Heat treatments and UV or infrared light can age a material artificially. The kinetic processes of material changes and the rate at which chemical and physical degradation occur inside the materials can be accelerated by applying heat. However, high-temperature heat treatments do not occur under normal weather circumstances. Thermal insulation materials are typically artificially aged by heat treating them at 70 °C for longer. Furthermore, high temperatures below the substance's melting point can also forecast long-term performance and usefulness [17,18].

3. Results and discussion

3.1. Heat treatment of the samples

Three pieces of Pyrogel samples were heat-treated and thermally aged for 24 h at 150 and 250 °C temperatures in a Venticell 111 drying apparatus in the air at 0 % humidity. Samples can be dried, desiccated, or heated to 300 °C with this apparatus. The laboratory drying oven has a chamber volume of 111 L and a temperature range of 10 °C above ambient to 250/300 °C. Its forced air circulation system ensures uniform temperature distribution during drying, heating, and sterilization. Its high operation comfort, precise temperature control, and short chamber temperature equalization times after door opening contribute to faster and more accurate tempering. The following tests were conducted following the heat treatments.

3.2. Thermal conductivity and specific heat capacity measurements

The thermophysical characteristics of the Pyrogel insulations were assessed after they were heat treated (aged) for a day at 150 and 250 °C. We investigated the alterations in structural and thermal characteristics and any potential connections between them throughout the measurements. We utilized unique measuring techniques that thoroughly disclosed the temperature-induced alterations of the examined samples. Since the results forecast the lifespan of the insulation material used in industrial settings, we view them as essential from an application standpoint. Three different samples from each material were tested before and after thermal annealing. Firstly, the thermal conductivity of the samples was measured after drying them at 70 °C, and then the samples were thermally aged (treated) at 150 and 250 °C for 1 day. New samples were used for all heat treatment and thermal conductivity measurements. The thermal conductivity and specific heat capacity were measured with the Netzsch HFM446 equipment at 10 °C mean temperature with a 20 °C temperature difference. This equipment is accurate, and its use is widespread in building physics. In Table 2, the measurement results are collected. In Table 2, we collected the uncertainties of the thermal conductivities (U_TC), specific heat capacity (U_C) and densities (U_D) provided by the equipment. The pyrogel samples' thermal conductivity increases from 0.0205 to 0.0214 W/mK after annealing at 150 °C, while it remains constant after a further heat treatment at 250 °C. Parallel to this, the specific heat capacity continuously increases with the annealing temperature.

As possible, structural change, crystallization, or surface oxidation can cause the modification of the thermal properties.

Photo images were taken from the materials before and after thermal annealing, see Fig. 1. One can see that the surface color gets darker and darker after thermal annealing. The change can be attributed to surface oxidation processes. We can also state from Fig. 1 that the color of the pyrogel gets darker only after thermal annealing at 250 °C. Notably, the material suffered an intensive change in color after thermal treatment but did not change its thermal conductivity between 150 and 250 °C. From this, it can be concluded that

Table 2
Thermal conductivity and specific heat capacity measurement results.

	Pyrogel 0			Pyrogel 150			Pyrogel 250		
Measurement mean temperature [°C]	Lambda [W/mK]	C [J/kgK]	Density [kg/m^3]	Lambda [W/mK]	C [J/kgK]	Density [kg/m^3]	Lambda [W/mK]	C [J/kgK]	Density [kg/m^3]
10	0.0205	834	205	0.0214	849	210	0.0214	882	214.7
U_TC [%]	2.45			2.33			2.33		
U_SH [%]		2.50			2,3			1,98	
U_D [%]			1.56			1.6			1.56
Percental change [%]				***105***	***102***		***105***	***106***	

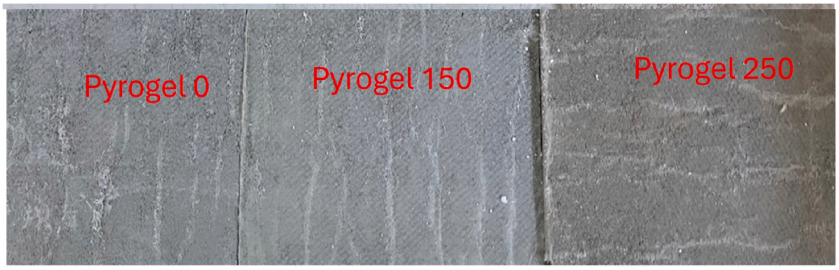

Fig. 1. Photo images from the samples.

the change in thermal conductivity due to the heat treatment is not entirely related to surface oxidation but to the change in the structure (crystalline or amorphous). We executed several physical and spectroscopical measures to describe the macroscopic changes.

3.3. The thermal properties of the materials

3.3.1. Thermal diffusivity

Diffusion, effusivity, or inertia are important thermal factors for single or multi-layered wall systems and thermal conductivity in transitory situations. Temporal and spatial temperature fluctuations and the temperature equalization rate are determined by thermal diffusivity. Thermal conductivity characterizes stable heat transport processes, whereas thermal diffusivity is transient. The thermal diffusion factor, the temperature conductivity factor or thermal diffusivity, is caused by an imbalance in temporal and spatial temperature distribution. It constantly influences the heat flow density. A sizeable thermal diffusivity causes a gradual temperature change.

$$D_T = \lambda/(\rho \times c) \quad \text{(Eq. 1)}$$

Calculating thermal diffusivity at constant pressure involves dividing thermal conductivity by density and specific heat capacity. It gauges how well a substance conducts heat energy and stores heat energy. High thermal diffusivity results in rapid heat transport. Heat moves swiftly through materials with high thermal diffusivity because they transport heat more quickly than the material's volumetric heat capacity, also known as "thermal mass."

In thermal diffusion, the elements mentioned above are combined to provide an equation quantifying a material's capacity to conduct and store heat energy. This measure is 'buffering' or thermal inertia, which results in increased conduction and decreased heat storage [47].

Fig. 2 shows that the thermal diffusivity of the pyrogel decreases by about 6 % after thermal annealing the sample at 250 °C. Any change could only be found after annealing at this temperature. If thermal conductivity increases, the insulation decreases. If the diffusivity increases, the insulation decreases. It must be mentioned that the errors were calculated from the uncertainties of the thermal conductivity, specific heat and density measurement results using the least squares method. These are also plotted in the figure. The uncertainties for the diffusivity values are 3.8, 3.62 and 3.43 % for the pyrogel samples not annealed and annealed at 150 and 250 °C (see Fig. 2).

3.3.2. Volumetric or effective heat capacity

$$V_c = \rho \times c \quad \text{(Eq. 2)}$$

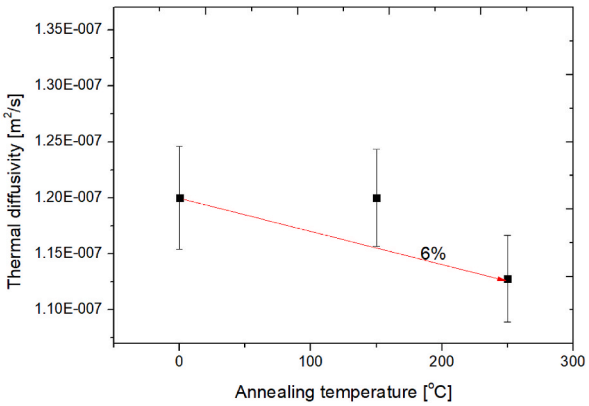

Fig. 2. Thermal diffusivity of the pyrogel material.

Volumetric heat capacity (V_c) is the multiplication of the material's density (ρ) and specific heat capacity (c), presented by Eq. (2). Fig. 3 shows that the heat capacity changes by about 4 % and 10 % after thermal annealing the samples at 150 and 250 °C, respectively [47].

It must be mentioned that the errors were calculated from the uncertainties of the specific heat and density measurement results using the least squares method. The uncertainties for the volumetric heat capacity values are 2.94, 2.78 and 2.52 % for the pyrogel samples not annealed and annealed at 150 and 250 °C. These are also plotted in Fig. 3.

We compared our results with results published earlier, where the authors investigated the changes in thermal properties of slentex arogel after heat treatment.

The thermal diffusivity changed from 1.06E-7 to 9.9E-8 after annealing at 150 °C, while the volumetric heat capacity increased by 15 % after annealing at 150 °C [45].

As previously stated, there is a discernible inverse relationship between a solid's density and specific heat capacity per mass since the bulk density of a solid chemical composition is closely linked to its molar mass and (mean) molar volume. Any given solid molar volume and total heat capacity are positively correlated due to the constancy of atomic volume and molar-specific heat capacity.

The molar volumes and, more consistently, the molar heat capacities of most solids are approximately constant. The Dulong-Petit specific heat capacity relation's volume-specific implication dictates that all elements' atoms must, on average, occupy the same volume in a solid; however, this is not always the case, with most variations resulting from variations in solid structural phases (amorphous or crystalline).

Thermal diffusivity is the ratio of the material's and product's fundamental transport and storage characteristics, and heat emission is a related number. Diffusion is mainly mentioned in the heat equation, a conservation of energy equation that gauges how quickly a body approaches thermal equilibrium. On the other hand, when a body is exposed to an intermittent or similarly disruptive forcing function, its effusivity—also referred to as inertia, accumulation, or reactivity—is its capacity to withstand temperature change.

Reaching the system's equilibrium condition many times takes longer when the volumetric heat capacity is more prominent. It is occasionally possible to apply the cautious analogy of thermal inertia to inertial behaviours seen in other engineering and science fields. The change in heat capacity is more impressive in the amorphous form than in the crystalline form [61–63].

We can also mention here that the materials in an amorphous state have better thermal insulation capability but differ based on their atomic composition. Their chemical and physical properties characterize both, but the main difference is in their structure. Compared to crystalline materials, amorphous solids are less brittle and more malleable. Solids without crystals are more pliable than those without crystals. The solid particle arrangement in amorphous materials is asymmetrical. There aren't equivalent interparticle forces between them.

3.4. X-ray diffraction measurement results

Fig. 4 shows the changes in the structure of the samples before and after heat treatment. Some interesting findings can be concluded. Due to the heat treatment, one can conclude that the samples undergo a re-crystallization process. The process can be attributed once to some peaks' horizontal shifting and well-visible changes in intensity. Interestingly, near 20°, some new peaks appear for the sample annealed at 150 °C. Moreover, these peaks disappear, and the amorphous peak will be more expressive after further annealing.

3.5. DSC experiment results

We can conclude from the differential scanning calorimetry measurement results that there are changes in the samples after heat treatment. Fig. 5 presents a glass transition region between 30 and 70 °C, and then a slight peak is observable, possibly representing a slight crystallization (150 °C).

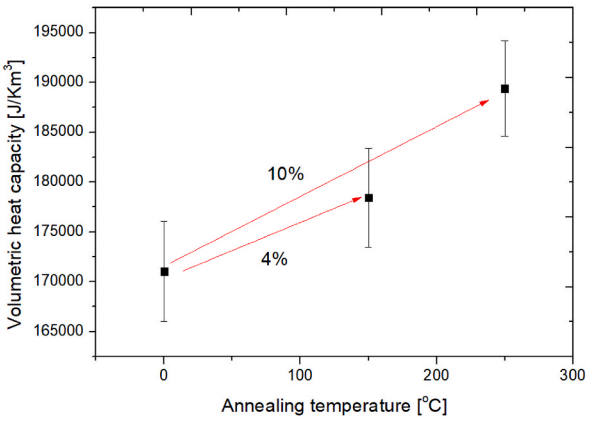

Fig. 3. Effective/volumetric heat capacity of the tested materials.

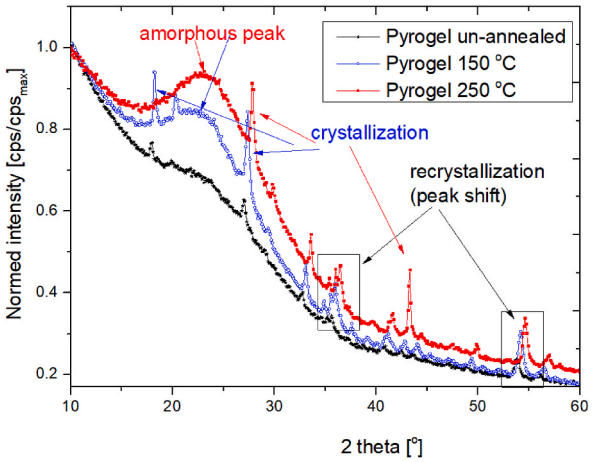

Fig. 4. X-ray diffraction measurement results.

It is also visible from Fig. 5 that, from 220 to 270 °C, a strong melting peak can be found. We also detected specific heat changes between 70 and 150 °C and between 200 and 250 °C, 1010 and 5340 J/kgK, respectively; the first belongs to an exothermic process, and the second belongs to an endothermic process [44].

3.6. Modifications in the bond structure of the samples

It was shown earlier that the samples' thermal conductivity and specific heat slightly increase to different extents due to heat treatment. However, the chemical composition has not changed significantly, but some amorphization and crystallization have coincided in their structure.

Systematic IR and Raman spectroscopy measurements were performed to better understand the changes in their bond structures due to heat treatment, which resulted in differences in their thermal parameters compared to their initial states.

3.6.1. Results of Fourier-transform infrared spectroscopy (FT-IR) and Raman spectroscopy measurements

Representative FT-IR spectra are shown in Fig. 6. The intensive peaks attributed to the amorphous silica aerogel and glass fibre components are present in the spectra of all samples. The most informative of these regarding the heat treatment-induced structural changes are as follows. The stretching vibration of the Si-O bond yields a characteristic intensive peak at ca. 1050 cm^{-1}, while the peak at 957 cm^{-1} is attributed in the literature to the localized modes of the stretching vibrations of terminal Si-OH groups [64,65]. The vibrations of the ring structures composed of complete SiO_4 tetrahedrons yield a peak at 798 cm^{-1} [66]. The methylated organosilica components yield characteristic peaks at 1275 cm^{-1} and 2974 cm^{-1} due to the Si-C and CH_3 stretching vibrations, respectively [67]. The prominent, broad peak around 3400 cm^{-1} is the superposition of the vibration bands of the terminal silanol (Si-OH) groups and the stretching vibrations of the adsorbed water molecules. At the same time, at about 1635 cm^{-1}, it is more characteristic of the formerly mentioned silanol groups [68,69].

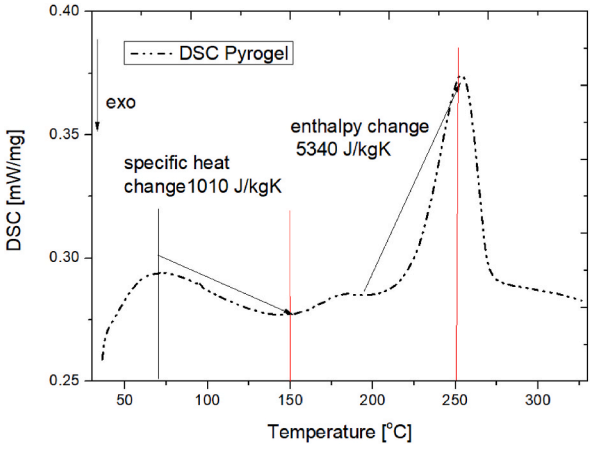

Fig. 5. DSC experiment results.

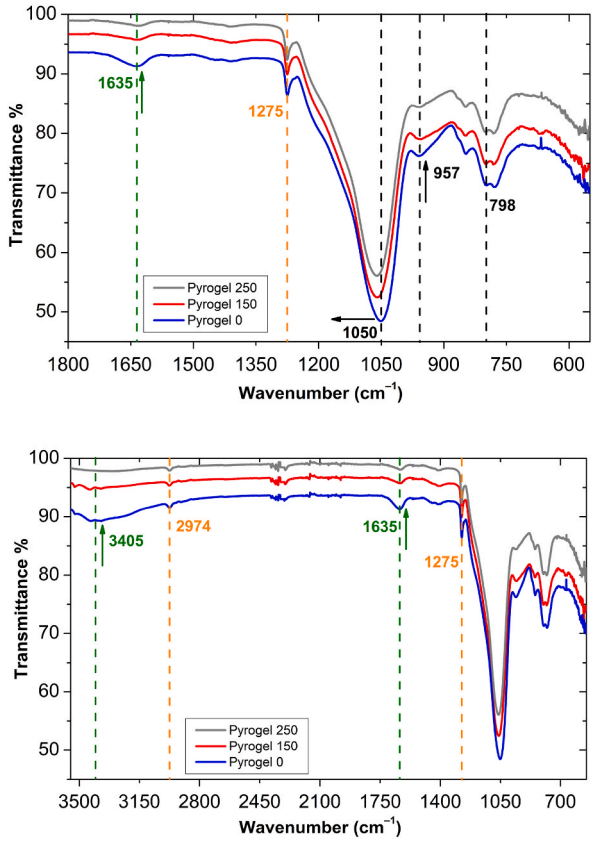

Fig. 6. Representative FT-IR spectra of untreated and heat-treated Pyrogel samples. The spectra are horizontally shifted for clarity. The two panels show identical spectra in different wavenumber ranges.

Judging from the FT-IR, heat treatment does not affect the chemical bonding structure of the Si-CH_3 parts of the material at the applied temperatures [70]. Naturally, the composite structure is dehydrated, which is observable in the dramatic decrease of the peak at 3405 cm^{-1}. Besides dehydration, the number of the free Si-OH groups decreases dramatically, as seen in the diminishing of the peaks at 957 cm^{-1} and 1635 cm^{-1} [68,69,71,72]. The corresponding chemical modification of the silica aerogel structure is the condensation of the terminal Si-OH groups into Si-O-Si chains. The literature shows that at around 250 °C this chemical process is also accompanied by the (partial) glassification of the amorphous silica, resulting in the slight shift of the Si-O stretching peak from 1050 cm^{-1} to higher wavenumbers. On the nanostructure scale, this is reflected by the dramatic alteration of the pearl-necklace-like architecture of the primary silica particles building up the backbone of the aerogel. A sintering process occurs among the spherical silica nanoparticles that increase the area of interaction between the particles in the form of neck thickening at the attachment points [66]. This process has

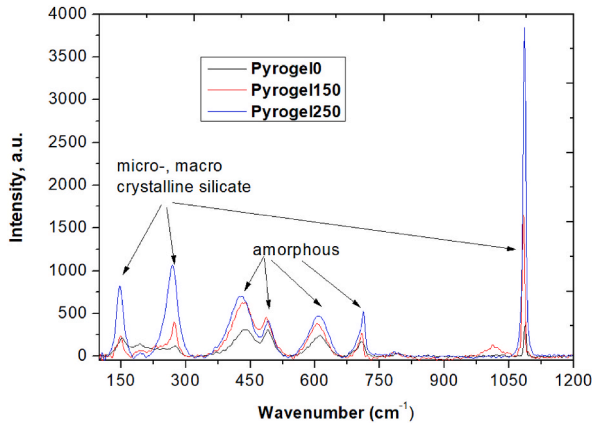

Fig. 7a. Raman spectra between 150 and 1200 cm^{-1} wavenumber.

intense consequences regarding the thermal properties of the material.

To acquire more understanding, the samples were investigated using Raman spectroscopy. Changes in the bond structures could be seen in the Raman spectra as well. The differences relate to the Si-O-Si and Si-O bonds. The transformation of amorphization, crystallization, and some other chemical reactions could be observed from the Raman spectra of the studied samples, see Fig. 7a and b.

The peaks connected with the micro-and macro crystalline structure of the silicate are:

147, 269, and 1087 cm^{-1}, whose peak intensity increases with heat treatment in the samples studied.

147 cm^{-1}: This peak is typically associated with low-frequency lattice vibrations. In silica aerogels, this can correspond to collective motions within the highly porous network, such as the crystalline microcrystalline structure.

269 cm^{-1}: Similarly, this peak is associated with lattice modes and can be observed in the aerogel structure due to the framework's flexibility, also connected with crystalline phases of Si-O-Si.

1087 cm^{-1}: This peak represents the symmetric stretching mode of Si-O bonds within the silicate tetrahedra connected with the crystalline phase.

While the following peaks connected with the amorphous form of the structure:

427, 492. 602 and 712 cm^{-1} also increase the intensity, but in a different manner, which agrees with the IR measurements.

427 cm^{-1}: This peak can be assigned to Si-O-Si bending vibrations within the aerogel's silicate network.

492 cm^{-1}: Also attributed to Si-O-Si bending modes, this peak is commonly found in both amorphous and aerogel silicates.

602 cm^{-1}: This peak is linked to symmetric stretching vibrations of the Si-O-Si bridges. Due to its porous nature, it may be less defined in aerogels than in dense amorphous silicates.

712 cm^{-1}: Associated with bending or rocking modes of Si-O-Si bonds, this peak is also present in aerogels but with broader characteristics due to the structure.

At the same time, the peaks connected with bond C-H are 2907 and 2967 cm^{-1}, the intensity of which changes decrease with time, which was well observed during IR measurements, too.

It could be seen that increasing peaks connected with amorphous and crystalline phases have a similar tendency from 0 to 150°. The change from 0 to 250 will be more significant for crystalline phases than amorphous ones. This is in good agreement or connection with the obtained heat conductivity values, which were more extensive for higher-temperature heat treatment [73–77].

To put all these into the frame, we can conclude that crystalline phases are more present in the material for the unannealed samples. Some crystalline peaks increase after annealing at 150 °C, and an amorphous signal increase is also noticeable. After further annealing at 250 °C, significant amorphous growth can be detected, with rearrangement of the crystalline phase, with local growth.

Some comments must be added: Solids have the highest heat capacity compared to liquids or gases. Gases have the lowest heat capacity because the intermolecular forces in solids and liquids are more substantial than in gases. For this reason, solids' specific heat capacity is higher than other forms of matter, and there are differences between amorphous and crystalline. The thermal insulation capability of the amorphous material is greater than that of the crystalline ones. They differ based on their atomic composition. Their chemical and physical properties characterize both, but the main difference is in their structure. Amorphous solids are softer and more pliable than crystalline ones and are not brittle. Amorphous solids are more flexible than crystalline ones. Amorphous solids' greater heat capacity than crystalline materials' at T ~10 K directly result from the extra vibrational modes around ωBP ~1 THz, often known as the boson peak (BP). When the material is crystalline, its thermal conductivity is higher than it is amorphous.

The particles that make up crystalline solids are organized in three dimensions. They have the same intermolecular forces. They have a distinct melting point and are anisotropic because it is easier to transport heat than in an amorphous substance. "Amorphous" means "formless." The solid particles of amorphous materials are arranged irregularly. They do not have equivalent intermolecular forces. Furthermore, the distance between the two particles varies. They do not have a specific geometric shape, which indicates that the material's internal heat pathway is more prolonged than in crystalline form.

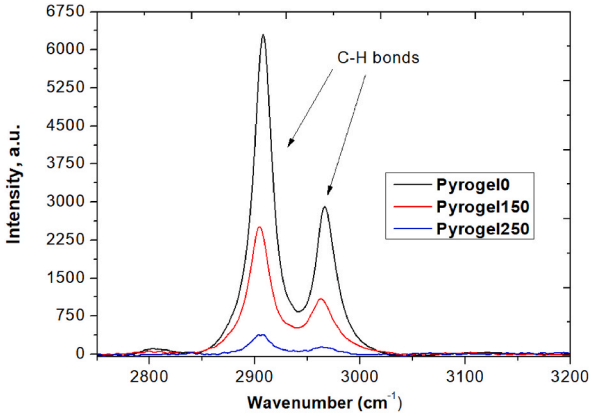

Fig. 7b. Raman spectra between 2700 and 3200 cm^{-1} wavenumbers.

3.7. Collection and comparison of the results

To summarize the key findings of our study, we created Table 3, where we collected all the tested thermal properties with their changes completed with our explanations. Moreover, the key results of the physical and chemical tests are also presented, supporting the explanations for the changes in the thermal properties.

3.7.1. Limitations of the investigations

As the paper was comprehensively presented, we showed that the pyrogel aerogel suffered changes in its thermal properties caused by thermal annealing and forced structural changes. We can find the novelty of the paper in its complexity and interdisciplinarity. We can emphasize that the investigations have limitations on the following. The experiments were executed in our laboratories, and the results were applied to this material after heat treatments at this temperature and time.

3.8. Environmental impact of aerogels

The production process of aerogels usually involves resources such as silica precursors and chemicals. Depending on the extraction methods and the availability of the resources, the extraction and processing of these resources can have environmental consequences. The sol-gel process and the manufacturing techniques of supercritical drying or freeze-drying can be energy-intensive, leading to greenhouse gas emissions and other environmental concerns.

Another consideration is waste generation. Although aerogels are light and highly porous, manufacturing produces waste by using them as a precursor or by-product. Proper waste management practices are essential to minimize environmental impact.

However, they are renowned for their durability and longevity, which can reduce the need for constant replacements and ultimately reduce the overall environmental impact. Some versions of aerogels are specifically biodegradable, which can be a more sustainable alternative than traditional insulating materials. These biodegradable aerogels naturally degrade over time, further reducing their environmental footprint.

Evaluating and comparing aerogel production's carbon footprint with other materials is vital to understand its environmental impact. Reducing carbon dioxide emissions associated with production processes can significantly contribute to environmental sustainability.

Furthermore, for aerogel manufacturers that operate according to environmental regulations and standards, it is essential to minimize the harmful effects of operations on the environment and surrounding communities.

In conclusion, although aerogels offer advantages such as excellent thermal insulation properties and durability, their environmental impact depends on various factors, including resource use, energy costs, waste generation, and end-of-life considerations. Continued efforts to improve manufacturing efficiency, reduce energy consumption, and develop end-of-life solutions are essential to lowering aerogels' environmental footprint.

4. Conclusions

In recent decades, aerogels have emerged as one of the most promising materials for thermal insulation. Aerogels possess remarkable qualities among super-insulating materials, including low density and thermal conductivity, tolerance to high temperatures, and transparency. Although this is a very pricey substance, its economic attractiveness can be increased by field incentives. The recently created materials exhibit exceptional insulating qualities. Aside from that, using aerogels reduces greenhouse gas emissions significantly since they have a favourable effect on the building's envelope's energy conservation. The need to increase building energy efficiency arises because the building sector uses a significant amount of the global energy consumed and released into the atmosphere. Thus, ideas like zero-emission buildings and passive homes are being presented. At the same time, using aerogels in vehicles such as airplanes, refrigerated trucks, and electric vehicles is justified due to their thin-film application potential.

Furthermore, industrial applications such as the insulation of district heating pipes or power plant pipelines should be considered due to their excellent heat resistance. Their use is also strongly recommended for the insulation of building services equipment. After being heat-treated (aged) for a day at 150 and 250 °C, the thermal characteristics of Pyrogel insulations were measured. We presented the changes in the thermal characteristics and structural changes observed in the measurements and investigated potential correlations between them. We discovered that pyrogel's thermal stability fluctuates beyond 150 °C; the heat capacity and diffusivity increase after thermal annealing. Both the results and the viewpoints of these are unique and new.

We can conclude, as the research goals of our paper, that the structural changes force the thermal annealing-induced thermal property change as follows:

- Thermal conductivity increases by 5 % after annealing at 150 °C, while it remains constant at further temperatures.
- Specific heat capacity: increases by 2 and 6 % after annealing at 150 C and 250 °C, respectively.
- Diffusivity: remains constant till 150 °C, changes (decreases) by about 6 % after annealing at 250 °C.
- Volumetric heat capacity: increases by 4 % and 10 % after annealing at 150 and 250 °C, respectively, since the heat storage capacity increases.

To support this, we performed physical and chemical characterization as follows:

Table 3
Collection of the measurement results and their understanding.

Thermal property and the methods	Not annealed	Annealed at 150 °C for 1 day	Annealed at 250 °C for 1 day
Thermal conductivity measurements [W/mK]	0.0205	0.0214 Increase (with 5 %)	0.0214 Remains of the previous
Explanation		Crystallyzation or re-crystalization should take place	recrystallization or amorphization should take place
Specific heat capacity [J/kgK]	834	849 Increase (with 2 %)	882 Increase (with 6 %)
Explanation		Crystallization should take place	Recrystallization should take place
Thermal diffusion [m^2/s]	1.2E-7	1.2E-7 Remains of the previous	1.12E-7 Decrease (with 6 %)
Explanation		Both thermal conductivity and specific heat increases this why in global the value remains constant	The high specific heat increase, decreases the diffusion
Volumetric heat capacity [J/Km^3]	171040	178437 Increase (with 4 %)	189392 Increase (with 10 %)
Explanation		The thermal insulation capability deteriorates	Heat storage capability increases
Reasons for the above changes			
XRD		Recrystallization, appearance of new peaks at 20°	Recrystallutaion – partial amorphization
DSC		Recrystallization	Strong peak appears in endothermic direction as a peak of a partial melting – showing amorphization
IR-Raman	Some functional groups enhance heat conduction some other functional groups obstruct the heat diffusion	Structural changes such as recrystallization and amorphization	Structural changes as amorphization and recrystallination

- Differential Scanning Calorimetry: substantial changes were found related to structural rearrangement. It showed recrystallization and partial amorphization after heat treatment.
- X-ray diffraction: the results show recrystallization and amorphization processes. Crystallization enhances thermal conduction, and amorphization enhances thermal insulation capability.
- FT-IR and Raman spectroscopies: micro-macro crystallization with amorphous phase chemical modifications can be concluded. Identification of both functional groups enhances heat conduction, and some others obstruct heat transfer. Moreover, recrystallization and amorphization were deduced too.

We can say that the thermal properties of the pyrogel material change differently depending on the annealing temperature.

As the paper was comprehensively presented, we showed that the pyrogel aerogel suffered changes in its thermal properties caused by thermal annealing and forced structural changes. We can find the novelty of the paper in its complexity and interdisciplinarity. We can emphasize that the investigations have limitations on the following. The experiments were executed in our laboratories, and the results were applied to this material after heat treatments at this temperature and time. In the future, we plan to examine the material from LCA analysis. Moreover, we will continue the work by analyzing other stress factors such as moisture exposure, mechanical load, or prolonged environmental exposure.

Our results can help designers and planners at the early stages of the design process. Moreover, it can help researchers interested in insulation materials as a starting point. Furthermore, we can conclude that tested materials are the perfect insulation option under these conditions.

CRediT authorship contribution statement

Ákos Lakatos: Writing – review & editing, Writing – original draft, Validation, Supervision, Project administration, Methodology, Investigation, Funding acquisition, Data curation, Conceptualization. **Attila Csík:** Writing – review & editing, Writing – original draft, Methodology, Investigation, Data curation. **Petra Herman:** Writing – review & editing, Writing – original draft, Methodology, Investigation, Data curation. **István Csarnovics:** Writing – review & editing, Writing – original draft, Methodology, Investigation, Formal analysis, Data curation.

Declaration of competing interest

The authors declare that they have no known competing financial interests or personal relationships that could have appeared to influence the work reported in this paper.

Acknowledgments

Project no. TKP2021-NKTA-34 has been implemented with the support provided by the Ministry of Innovation and Technology of Hungary from the National Research, Development and Innovation Fund, financed under the TKP2021-NKTA funding scheme. We specially thank the advices of József Kalmár from HUN-REN-DE Mechanisms of Complex Homogeneous and Heterogeneous Chemical Reactions Research Group, Department of Inorganic and Analytical Chemistry, University of Debrecen, Egyetem tér 1, Debrecen H-4032, Hungary.

Data availability

Data will be made available on request.

References

[1] U. Berardi, Aerogel-enhanced systems for building energy retrofits: insights from a case study, Energy Build. 159 (2018) 370–381.
[2] H.S. Khan, R. Paolini, P. Caccetta, M. Santamouris, On the combined impact of local, regional, and global climatic changes on the urban energy performance and indoor thermal comfort—the energy potential of adaptation measures, Energy Build. 267 (2022) 112152.
[3] L. Moga, L.I. Moga, Heat loss coefficient influence on the energy performance of buildings. Indoor Air 2014 – Proceedings of the 13th International Conference on Indoor Air Quality and Climate, 2014, pp. 299–306. ISBN 978-1-64339-731-5.
[4] S. Hámori, F. Kalmár, Hydraulic balancing analysis of a central heating system with constant supply temperature, EEMJ. 13 (11) (2014) 2789–2795.
[5] F. Kalmár, B. Bodó, B. Li, T. Kalmár, Decarbonization potential of energy used in detached houses—case study, Buildings 14 (6) (2024) 1824, https://doi.org/10.3390/buildings14061824.
[6] F. Kalmár, S. Hámori, Investigation of unbalancing problems in central heting systems, in: EXPRES 2015 : 7th International Symposium on Exploitation of Renewable Energy Sources and Efficiency, Cikos Stampa, Subotica, 2015, pp. 7–12.
[7] M.A. William, M.J. Suárez-López, S. Soutullo, M.M. Fouad, A.A. Hanafy, Enviro-economic assessment of buildings decarbonization scenarios in hot climates: mindset toward energy-efficiency, Energy Rep. 8 (Nov. 2022) 172–181, https://doi.org/10.1016/j.egyr.2022.05.164.
[8] M.K. Dixit, Life cycle embodied energy analysis of residential buildings: a review of literature to investigate embodied energy parameters, Renew. Sustain. Energy Rev. 79 (October 2016) (2017) 390–413, https://doi.org/10.1016/j.rser.2017.05.051.
[9] Mohsin Raza, Ayda Farhan, Basim Abu-Jdayil, Lignocellulose−based insulation materials: a review of sustainable and biodegradable solutions for energy efficiency, Int. J. Thermofluid. 24 (2024) 100844, https://doi.org/10.1016/j.ijft.2024.100844. ISSN 2666-2027.
[10] R. Larivière-Lajoie, P. Blanchet, B. Amor, Evaluating the importance of the embodied impacts of wall assemblies in the context of a low environmental impact energy mix Build, Environ. Times 207 (2022) 108534.
[11] E. Cintura, L. Nunes, B. Esteves, P. Faria, Agro-industrial wastes as building insulation materials: a review and challenges for Euro-Mediterranean countries Ind, Crop Prod. 171 (2021) 113833.
[12] A. Ali, A. Issa, A. Elshaer, A comprehensive review and recent trends in thermal insulation materials for energy conservation in buildings, Sustainability 16 (20) (2024) 8782, https://doi.org/10.3390/su16208782.
[13] L.D. Hung Anh, Z. Pásztory, An overview of factors influencing thermal conductivity of building insulation materials, J. Build. Eng. 44 (2021) 102604 [Google Scholar].
[14] T. Rymar, H. Tatarchenko, O. Fomin, V. Píštěk, P. Kučera, M. Beran, O. Burlutskyy, The study of manufacturing thermal insulation materials based on inorganic polymers under microwave exposure, Polymers 14 (2022) 3202 [Google Scholar].
[15] R. Hanaishy, A. Khader, Reducing carbon footprint by using thermal insulation materials in Palestinian buildings, An-Najah Univer. J. Res. - A (Nat. Sci.) 39 (1) (2025), https://doi.org/10.35552/anujr.a.39.1.2267.
[16] K. Wu, Q. Zhou, J. Cao, Z. Qian, B. Niu, D. Long, Ultrahigh-strength carbon aerogels for high temperature thermal insulation, J. Colloid Interface Sci. 609 (2022) 667–675.
[17] Á. Lakatos, Stability investigations of the thermal insulating performance of aerogel blanket, Energy Build. 185 (2019) 103–111.
[18] Á. Lakatos, Thermal insulation capability of nanostructured insulations and their combination as hybrid insulation systems, Case Stud. Therm. Eng. 41 (2023) 102630.
[19] Mariusz Kucharek, William MacRae, Liu Yang, Investigation of the effects of silica aerogel particles on thermal and mechanical properties of epoxy composites, Compos.part A Appl. Sci. Manuf. 139 (2020) 106108, https://doi.org/10.1016/j.compositesa.2020.106108. ISSN 1359-835X.
[20] Z. Li, X. Cheng, S. He, X. Shi, L. Gong, H. Zhang, Aramid fibers reinforced silica aerogel composites with low thermal conductivity and improved mechanical performance, Compos. Appl. Sci. Manuf. 84 (2016) 316–325.
[21] J. Jaxel, G. Markevicius, A. Rigacci, T. Budtova, Thermal superinsulating silica aerogels reinforced with short man-made cellulose fibers, Compos. Appl. Sci. Manuf. 103 (2017) 113–121.
[22] Keyang Cui, Haining You, Tingshan Huang, Linghao Peng, Wenyu Zhang, Zhuo Chen, Tao Mei, Qinghua Zhao, Dong Wang, Polyurethane-reinforced recycled aramid aerogels: multifunctional applications, Compos. Commun. (2024) 102199, https://doi.org/10.1016/j.coco.2024.102199. ISSN 2452-2139.
[23] Y. Luo, L. Yu, J. Men, J. Feng, Y. Jiang, L. Li, G. Qin, J. Feng, Ultralow thermal conductivity of single-atom doped carbon aerogel synthesized with a facile ambient-pressure-drying strategy, Carbon 213 (2023) 118167.
[24] Jing Men, Guojie Zhang, Junzong Feng, Yonggang Jiang, Liangjun Li, Yijie Hu, Jian Feng, Synthesis of near net-shape carbon aerogel composites for high-temperature thermal insulators with complex structures, Ceram. Int. (2024), https://doi.org/10.1016/j.ceramint.2024.12.321. ISSN 0272-8842.
[25] S. Korkmaz, İ.A. Kariper, Graphene and graphene oxide based aerogels: synthesis, characteristics and supercapacitor applications, J. Energy Storage 27 (2020) 101038, https://doi.org/10.1016/j.est.2019.101038.
[26] Akbar Firoozi Ali, Asghar Firoozi Ali, Ahmed A. El-Abbasy, Khaled Aati, Enhanced perspectives on silica aerogels: novel synthesis methods and emerging engineering applications, Result. Eng. 25 (2025) 103615. ISSN 2590-1230.
[27] X. Gu, Y. Ling, Research progress of aerogel materials in the field of construction, Alex. Eng. J. 91 (2024) 620–631, https://doi.org/10.1016/j.aej.2024.02.039.
[28] S. Krzemińska, A. Greszta, A. Różański, M. Safandowska, M. Okrasa, Effects of heat exposure on the properties and structure of aerogels for protective clothing applications, Microporous Mesoporous Mater. 285 (2019) 43–55, https://doi.org/10.1016/j.micromeso.2019.04.052.
[29] T. Li, H. Sun, M. Yang, C. Zhang, S. Lv, B. Li, L. Chen, D. Sun, All-Ceramic, compressible and scalable nano ibrous aerogels for subambient daytime radiative cooling (Open Access), Chem. Eng. J. 4 (452) (2023) 139518.
[30] H. Liu, X. Zhang, Y. Liao, J. Yu, Y.-T. Liu, B. Ding, Building-envelope-inspired, thermomechanically robust all-fiber ceramic meta-aerogel for temperature-controlled dominant infrared camouflage, Adv. Mater. 36 (25) (2024) 2313720. Cited 4 times.
[31] C. Yu, D. Lin, J. Guo, K. Zhuang, Y. Yao, X. Zhang, X. Jiang, Ultralight three-layer gradient-structured MXene/reduced graphene oxide composite aerogels with broadband microwave absorption and dynamic infrared camouflage, Small 20 (36) (2024) 2401755.
[32] C. Buratti, E. Belloni, F. Merli, M. Zinzi, Aerogel glazing systems for building applications, Rev. Energ. Build. 231 (2021) 110587, https://doi.org/10.1016/j.enbuild.2020.110587.

[33] C. Buratti, E. Moretti, Nanogel windows, in: F.P. Torgal, M. Mstretta, A. Kaklauskas, C.G. Granqvist, L.F. Cabeza (Eds.), Nearly Zero Energy Building Refurbishment, A Multidisciplinary Approach, Springer, London, 2013, pp. 555–581.
[34] H. Wang, H. Wu, Y. Ding, J. Feng, S. Wang, Feasibility and optimization of aerogel glazing system for building energy efficiency in different climates, Int. J. Low Carbon Technol. (2014) 1–8.
[35] C. Buratti, E. Moretti, M. Zinzi, High energy-efficient windows with silica aerogel for building refurbishment: experimental characterization and preliminary simulations in different climate conditions, Buildings 7 (2017) 1–12.
[36] Y. Rahimzadeh Chiya, Salih Mohammed Ahmed, Azeez A. Barzinjy, Microstructure characterizations, thermal analysis, and compression stress–strain behavior of lime-based plaster, Constr. Build. Mater. 350 (2022) 128921, https://doi.org/10.1016/j.conbuildmat.2022.128921. ISSN 0950-0618.
[37] C.Y. Rahimzadeh, A. Salih Mohammed, A.A. Barzinjy, Microstructure and chemo-physical characterizations, thermal properties, and modeling of the compression stress-strain behavior of lime-based roof and screed paste, Europ. J. Environ. Civil Eng. 27 (12) (2022) 3722–3742, https://doi.org/10.1080/19648189.2022.2150321.
[38] Y. Rahimzadeh Chiya, Salih Mohammed Ahmed, Azeez A. Barzinjy, Effect of temperature on the internal components including portlandite, weight loss, and compression stress-strain behavior of lime-based roof and screed paste, J. Build. Eng. 69 (2023) 106247, https://doi.org/10.1016/j.jobe.2023.106247. ISSN 2352-7102.
[39] H.P. Ebert, Thermal properties of aerogels, in: A. Aegerter, N. Leventis, M. Koebel (Eds.), Aerogels Handbook, Springer, New York, NY, USA, 2011, pp. 537–564.
[40] H. Song, W. Xiya, Z. Xiaoqian, S. Junwei, T. Fuliang, G. Saiping, D. Haipeng, L. Ping, H. Yajun, Preparation and properties of thermal insulation coating based on silica aerogel, Energy Build. 298 (2023) 113556. ISSN 0378-7788.
[41] U. Heineman, Annex 65 long-term performance of super-insulating-materials in building components and 586 systems, Rep. Subtask I: State Art Case Studies, EBC Annex 65 (2020).
[42] R. Coquard, D. Baillis, Thermal conductivity of Kelvin cell cellulosic aerogels: analytical and Monte Carlo approaches, J. Mater. Sci. 52 (19) (2017) 11135–11145.
[43] R. Galliano, K.G. Wakili, Th Stahl, B. Binder, B. Daniotti, Performance evaluation of aerogel-based and perlite-based prototyped insulations for internal thermal retrofitting: HMT model validation by monitoring at demo scale, Energy Build. 126 (2016) 275–286.
[44] Z. Kovács, A. Csík, Á. Lakatos, Thermal stability investigations of different aerogel insulation materials at elevated temperature, Therm. Sci. Eng. Prog. 42 (2023) 101906.
[45] Á. Lakatos, A. Trník, Thermal diffusion in fibrous aerogel blankets, Energies 13 (4) (2020) 823, https://doi.org/10.3390/en13040823.
[46] M. Puttavva Meti, D.B. Mahadik, K.Y. Lee, Q. Wang, K. Kanamori, Y.D. Gong, H. H- Park, Overview of organic–inorganic hybrid silica aerogels: progress and perspectives, Mater. Des. 222 (2022) 111091.
[47] Á. Lakatos, A. Csík, I. Csarnovics, Experimental verification of thermal properties of the aerogel blanket, Case Stud. Therm. Eng. 25 (2021) 100966.
[48] Á. Lakatos, I. Csarnovics, Influence of thermal annealing on structural properties of silica aerogel super insulation material, J. Therm. Anal. Calorim. 142 (1) (2020) 321–329.
[49] F. Spiske, M.P. Dirauf, A.S. Braeuer, Aerogel-lined capillaries for Raman signal gain of aqueous mixtures, Sensors 22 (12) (2022) 4388, https://doi.org/10.3390/s22124388.
[50] T. Woignier, J.L. Sauvajol, J. Pelous, R. Vacher, Aerogel to glass transformation studied by low frequency Raman scattering, J. Non-Cryst. Solids 121 (Issues 1–3) (1990) 206–210, https://doi.org/10.1016/0022-3093(90)90133-7. ISSN 0022-3093.
[51] Y. Song, B. Li, S. Yang, et al., Ultralight boron nitride aerogels via template-assisted chemical vapor deposition, Sci. Rep. 5 (2015) 10337, https://doi.org/10.1038/srep10337.
[52] Y.M. Volfkovich, A.S. Lobach, N.G. Spitsyna, et al., Hydrophilic and hydrophobic pores in reduced graphene oxide aerogel, J. Porous Mater. 26 (2019) 1111–1119, https://doi.org/10.1007/s10934-018-0712-2.
[53] R. Stangl, W. Platzer, V. Wittwer, IR emission spectroscopy of silica aerogel, J. Non-Cryst. Solids 186 (1995) 256–263, https://doi.org/10.1016/0022-3093(95)00050-X. ISSN 0022-3093.
[54] Ashraf M. Alattar, Spectral and structural investigation of silica aerogels properties synthesized through several techniques, J. Non-Cryst. Solids 571 (2021) 121048, https://doi.org/10.1016/j.jnoncrysol.2021.121048. ISSN 0022-3093.
[55] M. Kaya, A. Tabak, Recycling of an agricultural bio-waste as a novel cellulose aerogel: a green Chemistry study, J. Polym. Environ. 28 (2020) 323–330, https://doi.org/10.1007/s10924-019-01609-6.
[56] Y. Lu, X. Li, X. Yin, H. Utomo, N. Tao, H. Huang, Silica aerogel as super thermal and acoustic insulation materials, J. Environ. Protect. 9 (2018) 295–308, https://doi.org/10.4236/jep.2018.94020.
[57] https://www.aerogel.com/product/pyrogel-xte/.
[58] I. Turhan Kara, B. Kiyak, N. Colak Gunes, et al., Life cycle assessment of aerogels: a critical review, J. Sol. Gel Sci. Technol. 111 (2024) 618–649, https://doi.org/10.1007/s10971-024-06455-0.
[59] Á. Lakatos, A. Csík, Multiscale thermal investigations of graphite doped polystyrene thermal insulation, Polymers (Basel) 14 (8) (2022 Apr 14) 1606, https://doi.org/10.3390/polym14081606. PMID: 35458356; PMCID: PMC9031919.
[60] Hans Simmler, Samuel Brunner, Ulrich Heinemann, Hubert Schwab , Kumar Kumaran, Phalguni Mukhopadhyaya , Daniel Quénard, Hébert Sallée , Klaus Noller, Esra Kücükpinar-Niarchos, Martin Tenpierik, Hans Cauberg, Dr.Eicher+Pauli IEA/ECBCS Annex 39 Vacuum Insulation Panels - Study on VIP-Components and Panels for Service Life Prediction of VIP in Building Applications (Subtask A) - EMPA: Swiss Federal.
[61] C. Kittel, Introduction to Solid State Physics, eighth ed., 2005. ISBN 0-471-41526-X WIE ISBN 0-471-68057-5.
[62] Y. Yousefi, F. Tariku, Thermal conductivity and specific heat capacity of insulation materials at different mean temperatures, J. Phys.: Conf. Ser. (2021) 012090.
[63] Tao Gao, Bjørn Petter Jelle, Thermal conductivity of amorphous silica nanoparticles, J. Nano Res. 21 (2019) 108.
[64] J. Núñez, Y. Wang, S. Bäumer, A. Boersma, Inline infrared chemical identification of particulate matter, Sensors 20 (15) (2020) 4193, https://doi.org/10.3390/s20154193.
[65] M. Ocaña, V. Fornés, C.J. Serna, The variability of the infrared powder spectrum of amorphous SiO2, J. Non-Cryst. Solids 107 (Issues 2–3) (1989) 187–192.
[66] Plinio Innocenzi, Paolo Falcaro, David Grosso, Florence babonneau Order−Disorder transitions and evolution of silica structure in self-assembled mesostructured silica films studied through FTIR spectroscopy, J. Phys. Chem. B 107 (20) (2003) 4711–4717.
[67] D.B. Mahadik, H.-N.-R. Jung, Y.K. Lee, K.-Y. Lee, H.-H. Park, Elastic and superhydrophobic monolithic methyltrimethoxysilane-based silica aerogels by two-step sol-gel process, J. Microelectron. Packag. Soci. 23 (1) (2016) 35–39, https://doi.org/10.6117/KMEPS.2016.23.1.035.
[68] M. Decottignies, J. Phalippou, J. Zarzycki, Synthesis of glasses by hot-pressing of gels, J. Mater. Sci. 13 (1978) 2605–2618, https://doi.org/10.1007/BF02402747.
[69] Alessandro Bertoluzza, Concezio Fagnano, Maria Antonietta Morelli, Vittorio Gottardi, Massimo Guglielmi, Raman and infrared spectra on silica gel evolving toward glass, J. Non-Cryst. Solids 48 (1) (1982) 117–128.
[70] Rodrigo Brambilla, João H.Z. dos Santos, Márcia S.L. Miranda, Ray L. Frost, Thermal stability of octadecylsilane hybrid silicas prepared by grafting and sol–gel methods, Thermochim. Acta 469 (Issues 1–2) (2008) 91–97.
[71] M. Ocaña, V. Fornés, C.J. Serna, The variability of the infrared powder spectrum of amorphous SiO2, J. Non-Cryst. Solids 107 (Issues 2–3) (1989) 187–192.
[72] Carole C. Perry, Xiaochun Li, Structural studies of gel phases. Part 1.—infrared spectroscopic study of silica monoliths; the effect of thermal history on structure, J. Chem. Soc., Faraday Trans. 5 (1991).
[73] B. Riegel, I. Hartmann, W. Kiefer, J. Groβ, J. Fricke, Raman spectroscopy on silica aerogels, J. Non-Cryst. Solids 211 (3) (1997) 294–298.
[74] G. Reichenauer, Structural characterization of aerogels, in: M. Aegerter, N. Leventis, M. Koebel (Eds.), Aerogels Handbook. Advances in Sol-Gel Derived Materials and Technologies, Springer, New York, NY, 2011, https://doi.org/10.1007/978-1-4419-7589-8_21.

[75] K. Igarashi, K. Tajiri, Y. Tai, et al., Structural study by DSC, SAXS, and Raman spectroscopy of silica aerogel, Z. Physik D Atoms, Mol. Clust. 26 (Suppl 1) (1993) 207–209, https://doi.org/10.1007/BF01425666.
[76] T. Woignier, C. Fernandez-Lorenzo, J.L. Sauvajol, et al., Raman study of structural defects in SiO2 aerogels, J. Sol. Gel Sci. Technol. 5 (1995) 167–172, https://doi.org/10.1007/BF00487013.
[77] G.E. Walrafen, M.S. Hokmabadi, N.C. Holmes, W.J. Nellis, S. Henning, Raman spectrum and structure of silica aerogel, J. Chem. Phys. 82 (1985) 2472–2476, https://doi.org/10.1063/1.448292.